JOURNAL OF MATERIALS SCIENCE **34** (1999) 6183–6187

A dual-phase-lag diffusion model for interfacial layer growth in metal matrix composites

J. K. CHEN, J. E. BERAUN
Laser Effects Branch, Phillips Laboratory, Kirtland AFB, NM 87117, USA
D. Y. TZOU
Department of Mechanical and Aerospace Engineering, University of Missouri at Columbia, Columbia, MO 65211, USA

The time dependence of a reinforcement-matrix interfacial layer growth (RMILG) in most metal matrix composites (MMC's) is not $t^{1/2}$ as described by Fick's law. Moreover, the RMILG vs. $t^{1/2}$ could be linear for relatively short and long times, and an anomalous transition behavior exhibits in between. In this paper, a dual-phase-lag diffusion (DPLD) model is proposed to characterize the RMILG kinetics. Unlike Fick's law, it accounts for the two lagging times required for the processes of interdiffusion and chemical reaction. This unique feature empowers the DPLD model to capture the multiple stages response over the entire RMILG history. Model validation is verified with the experimental results of seven different MMC systems. © *1999 Kluwer Academic Publishers*

1. Introduction

Reinforcement-matrix interfacial layer growth (RMILG) has been observed in MMC's during service and, more commonly, during fabrication at elevated temperatures. The presence of an interfacial phase could affect the mechanical properties and physical integrity of the composite systems. Therefore, an understanding of the nature, kinetics and rate-controlling process for the RMILG is paramount. This will allow to possibly optimize joining temperature and time to form a joint, free from any deleterious second phases. Also, an accurate characterization of the joint evolution during fabrication and operation service will provide useful information for investigating the degraded system mechanical properties and physical integrity.

RMILG in MMC's depends upon composite material systems, joining process, operation temperatures, diffusion and chemical reaction, time, etc. The growth kinetics is usually studied from thickness measurements performed under the optical microscope on polished sections cut perpendicularly to the reinforcement direction. It has been reported that RMILG does not often follow Fickian diffusion law but is instead controlled by t^m ($m \neq 1/2$), for example, between SiC fibers and Titanium alloys [1–3], tungsten fibers and superalloys whose major contents include Fe, Ni and Co [4, 5], eta-aluminum fibers and magnesium alloys [6], and SiC particulates and Al-Ti alloys [7]. More specifically, the RMILG is controlled by variable m values for which the layer thickness (H) vs. $t^{1/2}$ is linear in some periods while nonlinear in others [1].

Besides curve-fitting methods, several analytical studies have examined the RMILG in MMC's. However, the fundamental framework for most of the investigations is based on Fick's law, i.e., $H \sim t^{1/2}$. Obviously, these Fick's law-based approaches are unable to describe the entire history of the RMILG, especially for the cases with multiple stages response.

The dual-phase-lag diffusion (DPLD) model has been proposed by the authors for investigating the rapid thermal oxidation in thin films [8] and intermetallic growth in solder joints [9]. Because this model considers the delayed response between the mass flux vector and density gradient, it is able to capture the anomalous transition behavior between the linear ($H \sim t^{1/2}$) and nonlinear response regimes. In [8] and [9], the DPLD model was established based on the planar condition. To characterize the RMILG in MMC's, a general, one-dimensional DPLD model is proposed in this paper. On account of the geometry of long fibers or particulates in an MMC, the model is based on the cylindrical and spherical coordinate systems. The derivation will be detailed in the following. Also, the model credibility will be verified with the experiment data of seven different MMC systems [1, 3, 5].

2. Phase-lag concept

The dual-phase-lagging to both the relative mass flux vector ($\bar{j}$) and density gradient ($\nabla\rho$) in an interfacial compound between two dissimilar materials is expressed as

$$\bar{j}(\bar{r}, t + \tau_j) = -D\nabla\rho(\bar{r}, t + \tau_\rho) \tag{1}$$

where $\bar{r}$ represents the position vector, t denotes time, τ_j and τ_ρ are the delayed times associated with $\bar{j}$ and $\nabla\rho$, respectively, and D is the diffusion coefficient. Equation 1 shows the temperature gradient established across a material volume located at a position vector $\bar{r}$ at time $t + \tau_\rho$ results in a mass flux to diffuse at a different instant of time $t + \tau_j$. The values of the two phase lags, τ_ρ and τ_j, depend upon composite material systems as well as environmental temperature. They are treated as two intrinsic properties characterizing the transient process of mass transport. To combine with the mass continuity equation, where all the physical quantities occur at the same instant of time, Equation 1 is rewritten in the first-order Taylor series expansion

$$\bar{j}(\bar{r}, t) + \tau_j \frac{\partial \bar{j}}{\partial t}(\bar{r}, t) \cong -D\nabla\rho(\bar{r}, t) - D\tau_\rho \frac{\partial}{\partial t}\nabla\rho(\bar{r}, t), \qquad \tau_j; \tau_\rho \ll t \quad (2)$$

The mass continuity equation for the interfacial compound is given by

$$-\nabla \cdot \bar{j}(\bar{r}, t) = \frac{\partial \rho}{\partial t}(\bar{r}, t) \quad (3)$$

The lagging response can be better understood by eliminating the mass flux vector from Equations 2 and 3. Taking the divergence of Equation 2 and then substituting Equation 3 into the result yields

$$\nabla^2\rho + \tau_\rho \frac{\partial}{\partial t}\nabla^2\rho = \frac{1}{D}\frac{\partial \rho}{\partial t} + \left(\frac{\tau_j}{D}\right)\frac{\partial^2 \rho}{\partial t^2} \quad (4)$$

Equation 4 clearly indicates that the diffusion coefficient, D, and the two phase lags, τ_j and τ_ρ, all play an important role in the mass transport. Note that a constant D is assumed in the above derivation.

Depending upon the values of τ_j and τ_ρ, three special cases are drawn from Equation 4. For the case of $\tau_j = \tau_\rho$, not necessarily equal to zero, Equation 4 simplifies to Fick's diffusion law. It is thus evident that an instantaneous response between the mass flux vector and density gradient is the intrinsic assumption behind Fick's law. With the conditions of $\tau_\rho = 0$ but $\tau_j \neq 0$, the second term on the left hand side of Equation 4 vanishes. This results in a wave equation with a mass transport speed of $(D/\tau_j)^{1/2}$ and a diffusion damping effect. The infinite growth rate at $t = 0$ in this case implies that an interfacial layer of finite thickness will instantaneously be formed at the very beginning of a joint process. Another special case is $\tau_j = 0$ but $\tau_\rho \neq 0$. For this case no interfacial compound is grown. The discussion of these three special cases can be found in Chen *et al.* [9].

3. One-dimensional DPLD model

An interfacial layer in MMC's results from a complicated process of interdiffussion and chemical reaction of the constituents in the two composite components. An interfacial compound could also consist of several sub-layers; each layer has different material phases. Because of the complex physics behind the interfacial phase formation, it is difficult to develop a model which is able to precisely describe the entire history and every detail process of the RMILG. To keep the analytical model as simple as possible, we propose an alternative, bulk diffusion model in which the interdiffusion process is equivalently considered as a one-way diffusion. With this assumption, diffusion will only occur from one material (which consists of diffusion controlling constituents) into the other (which is relatively inactive to diffuse). The total quantity of the constituents diffused, however, is the same as that resulting from the interdiffusion process. Despite the fact that the simplified approach could not virtually reflect the actual interfacial phase formation (for example, the reaction zone grows into both fibers and matrix), it will not lose its capability of predicting the overall interfacial layer thickness.

Assume that the cross-section of the reinforcement in an MMC is cylindrical for fibers and spherical for particulates. Due to the symmetry, it is reasonable to consider that the RMILG is a one-dimensional process and only takes place along the radial direction. Next, let ρ_o be the density of the diffused constituents in the diffusion-active material and ρ_s, the saturated density of the diffused constituents at the boundary between the interfacial layer and the diffusion-inactive material. Also let r be the radial coordinate originated from the center of the reinforcement and a, the initial radius of the reinforcement (Fig. 1). Thus the governing equation for this one-dimensional RMILG becomes, from Equation 4,

$$\frac{1}{r^\lambda}\frac{\partial}{\partial r}\left(r^\lambda \frac{\partial \rho}{\partial r}\right) + \tau_\rho \frac{\partial}{\partial t}\left[\frac{1}{r^\lambda}\frac{\partial}{\partial r}\left(r^\lambda \frac{\partial \rho}{\partial r}\right)\right] = \frac{1}{D}\frac{\partial \rho}{\partial t} + \left(\frac{\tau_j}{D}\right)\frac{\partial^2 \rho}{\partial t^2} \quad (5)$$

which is subject to the following boundary and initial conditions:

$$\rho = \rho_s \ \text{at}\ r = L(t) \equiv a + H(t); \quad \rho \to 0 \ \text{as}\ r \to \infty \quad (6)$$

and

$$\rho = 0, \quad \frac{\partial \rho}{\partial t} = 0, \quad L = a \ \text{at}\ t = 0 \quad (7)$$

In Equation 5, λ equals 1 or 2, depending on the geometry (cylindrical or spherical, respectively). Note that

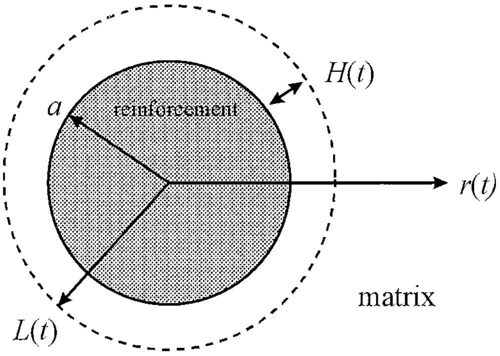

Figure 1 One-dimensional model for interfacial layer growth.

Equation 5 also represents the planar case, i.e., unidirectional diffusion, when $\lambda = 0$. In this case, a is the initial thickness of the diffusion-active material.

Once the density distribution of the diffused constituents in an interfacial compound is determined, the interlayer thickness can be estimated by using the surface recession rate [10]

$$\frac{d(\rho_o L)}{dt} = -D\frac{\partial \rho}{\partial r} \quad \text{at}\, r = L(t) \tag{8}$$

For convenience, let us define the dimensionless parameters as follows:

$$R \equiv \frac{\rho}{\rho_s}, \quad \beta \equiv \frac{t}{\tau_j}, \quad T \equiv \frac{\tau_\rho}{\tau_j}, \quad \xi \equiv \frac{r}{\sqrt{D\tau_j}}, \\ \gamma \equiv \frac{\rho_s}{\rho_o}, \quad \text{and} \quad l \equiv \frac{L}{\sqrt{D\tau_j}}, \tag{9}$$

The two governing Equations, 5 and 8, then, can be rewritten in the non-dimensional form

$$\frac{1}{\xi^\lambda}\frac{\partial}{\partial \xi}\left(\xi^\lambda \frac{\partial \rho}{\partial \xi}\right) + T\frac{\partial}{\partial \beta}\left[\frac{1}{\xi^\lambda}\frac{\partial}{\partial \xi}\left(\xi^\lambda\frac{\partial R}{\partial \xi}\right)\right] = \frac{\partial R}{\partial \beta} + \frac{\partial^2 R}{\partial \beta^2} \tag{10}$$

and

$$\frac{dl}{d\beta} = -\frac{\partial R}{\partial \xi} \quad \text{at}\, \xi = \gamma l(\beta) \tag{11}$$

Also the dimensionless boundary and initial conditions become

$$R = 1 \quad \text{at}\, \xi = \gamma l(\beta); \qquad R \to 0 \quad \text{as}\, \xi \to \infty \tag{12}$$

and

$$R = 0, \; \frac{\partial R}{\partial \beta} = 0, \; \text{and} \; l = \frac{a}{\gamma\sqrt{D\tau_j}} \quad \text{at}\, \beta = 0 \tag{13}$$

Laplace transform for Equations 10 and 11 can be obtained in a straightforward manner:

$$\xi^2\frac{d^2\bar{R}}{d\xi^2} + \lambda\xi\frac{d\bar{R}}{d\xi} - B^2\xi^2\bar{R} = 0 \tag{14}$$

and

$$p\bar{l} - \frac{a}{\gamma\sqrt{D\tau_j}} = -\frac{d\bar{R}}{d\xi} \tag{15}$$

in which p is the Laplace transform parameter, and B is defined as

$$B = \sqrt{\frac{p(1+p)}{1+Tp}} \; (\succ 0) \tag{16}$$

Equation 14 is a Bessel differential equation. The general solution is given by

$$\bar{R} = \xi^{\frac{1-\lambda}{2}}[C_1 I_\upsilon(\sqrt{-B}\xi) + C_2 K_\upsilon(\sqrt{-B}\xi)] \tag{17}$$

where I_υ and K_υ are the first and second modified Bessel functions of order υ, respectively, and $\upsilon = |(1-\lambda)/2|$.

3.1. Fiber-reinforced MMC's

For a fiber-reinforced MMC, $\lambda = 1$. Equation 17 thus becomes

$$\bar{R} = C_1 I_o(B\xi) + C_2 K_o(B\xi) \tag{18}$$

The sum of H and a in the Laplace transform domain ($\bar{l}$) can be obtained from the transformed growth kinetics (Equation 15) and the boundary conditions (Equations 12 and 13)

$$p\left(p\bar{l} - \frac{a}{\gamma\sqrt{D\tau_j}}\right)K_o(B\gamma p\bar{l}) = BK_1(B\gamma p\bar{l}) \tag{19}$$

Note that the above equation is transcendental; therefore, a closed form solution for $\bar{l}$ cannot be derived.

3.2. Particulate-reinforced MMC's

The solution of Equation 17 can be simplified for a particulate-reinforced MMC by setting $\lambda = 2$

$$\bar{R} = \frac{1}{\xi}\left[C_1 e^{B\xi} + C_2 e^{-B\xi}\right] \tag{20}$$

Unlike fiber-reinforced MMC's, the closed form solution for $\bar{l}$ is obtained as

$$\bar{l} = \frac{\frac{a}{\sqrt{D\tau_j}}p + B\gamma + \sqrt{\left(\frac{a}{\sqrt{D\tau_j}}p + B\gamma\right)^2 + 4\gamma p}}{2\gamma p^2} \tag{21}$$

3.3. Simplified solutions

For $H \ll a$, it is reasonable to approximate the RMILG as an one-dimensional planar process. The solution of Equation 17 for the this case ($\lambda = 0$) is simple,

$$\bar{R} = C_1 e^{B\xi} + C_2 e^{-B\xi} \tag{22}$$

The interfacial layer thickness in the Laplace domain, $\bar{h}$, is then found to be

$$\bar{h} = \frac{1}{p^2}\sqrt{\frac{p(1+p)}{1+Tp}} \tag{23}$$

The widely used Fickian diffusion equation for the planar case can be reduced from Equation 23 by setting $T = 1$. This leads to

$$\bar{h} = \frac{1}{p^{3/2}} \tag{24}$$

The inverse of Equation 24 gives

$$h = \frac{2}{\sqrt{\pi}} \cdot \sqrt{\beta} \tag{25}$$

The well-known $t^{1/2}$ behavior in a Fickian diffusion process is thus retrieved.

Each of the three Equations, 19, 21 and 23, contains several branch points which prevent from obtaining an analytical inversion for the RMILG. Therefore, the well-proven Riemann-sum approximation for the Laplace inversion is adopted [11]

$$l(\beta) \cong \frac{e^{4.7}}{\beta}\left[\frac{1}{2}\bar{l}\left(\frac{4.7}{\beta}\right) + \mathrm{Re}\sum_{n=1}^{N}\bar{l}\left(\frac{4.7in\pi}{\beta}\right)(-1)^n\right] \tag{26}$$

where $\bar{l}$ is given in Equations 19 and 21 for the cylindrical and spherical cases, respectively, and is replaced with $\bar{h}$ in Equation 23 for the planar case; "Re" represents the real part of the summation. The number of terms N used in the Riemann-sum increases until a specified Cauchy norm for convergence is satisfied. In this work, the Cauchy norm is set to be smaller than 10^{-15}. Computer calculation of Equation 26 is simple and only requires a little effort.

4. Determination of the material parameters

By examining Equations 9, 19, 21 and 23, there are five material properties, τ_j, τ_ρ, D, ρ_o and ρ_s, and one geometry parameter, a, involved in the DPLD model. Nonetheless, five constants, τ_j, $T(= \tau_\rho/\tau_j)$, $\gamma(= \rho_s/\rho_o)$, $\sqrt{D\tau_j}$ and a, are needed to solve Equations 19 and 21 for the cylindrical and spherical cases, respectively. The required constants further reduce to three, i.e., τ_j, T and $\gamma\sqrt{D\tau_j}$ for the planar case (see Equation 23).

To determine these parameters, a tedious trail and error approach must be performed for the cylindrical and spherical cases. On the other hand, the three material parameters for the planar case can easily be calibrated and will be discussed in the following.

The asymptotic behaviors of Equation 23 can be analytically derived in terms of the physical quantities [9]

$$H \to \frac{\gamma\sqrt{D}}{\Gamma(3/2)T}\sqrt{t} \quad \text{as}\, t \to 0 \tag{27}$$

and

$$H \to \frac{2\gamma\sqrt{D}}{\sqrt{\pi}}\sqrt{t} \quad \text{as}\, t \to \infty \tag{28}$$

The above two equations show the RMILG is a function of $t^{1/2}$ at both extremely short and long times. However, the growth rates are different. Although the ratio T has nothing to do with the RMILG at relatively long time, it does significantly influence the growth rate for short time. It is seen from Equation 27 that the smaller the ratio, the greater the growth rate.

With the slope of the experimentally obtained H vs. $t^{1/2}$ curve at extremely long times, the value of $\gamma\sqrt{D}$ can be calculated by using Equation 28. Substituting this value into Equation 27, the ratio T is then estimated from the experimental data at the extremely short times. Another constant, τ_j, can simply be acquired by choosing a value with which the DPLD model fits the experimental data best. Thus, the values of τ_j, T and $\gamma\sqrt{D\tau_j}$ are all determined.

5. Results and discussion

Credibility of the proposed DPLD model for the RMILG in MMC's is validated with seven fiber composite systems. Because the radii of the fibers are much larger than the interfacial layer thickness, Equation 23 was employed in these calculations. Table I lists the values of the three material parameters. The predicted RMILG results are plotted as a function of $t^{1/2}$ in Figs 2–4.

Fig. 2 compares the data of Blue *et al.* [3] for the RMILG in SCS-6/β21S composites. Beta 21S is a titanium alloy having the composition Ti-15Mo-2.7Nb-3Al-0.25Si wt %. The SCS-6 fibers have an initial diameter of about 147 μm, with a 3-μm carbon-rich coating. The interfacial layer growth measurements were taken on 16-ply composite samples in the as-received, 1100 °C thermal cycled for 30-, 120-, and 300-s conditions [3]. The dashed line is predicted by Blue *et al.*

TABLE I Material parameters of MMC's

MMC	τ_j (h)	Z	$\gamma\sqrt{D\tau_j}$ (μm^{-1})
SCS-6//β21S	10.0	2.0	0.34.
SiC/Ti-6Al	200.0	0.50	13.04
SiC/Ti	250.0	0.17	16.58
SS316	65.0	0.05	10.66
Incoloy 907	75.0	0.025	8.70
FeCrAlY	500.0	5.0	51.57
Waspaloy	15.0	7.0	1.81

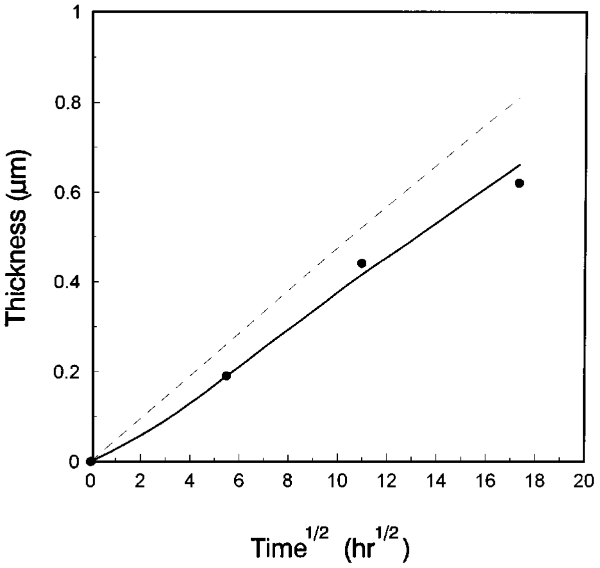

Figure 2 Interfacial layer growth in SCS-6/β21S MMC. (●) Experiment [3], (- -) Prediction [3], (—) DPLD model.

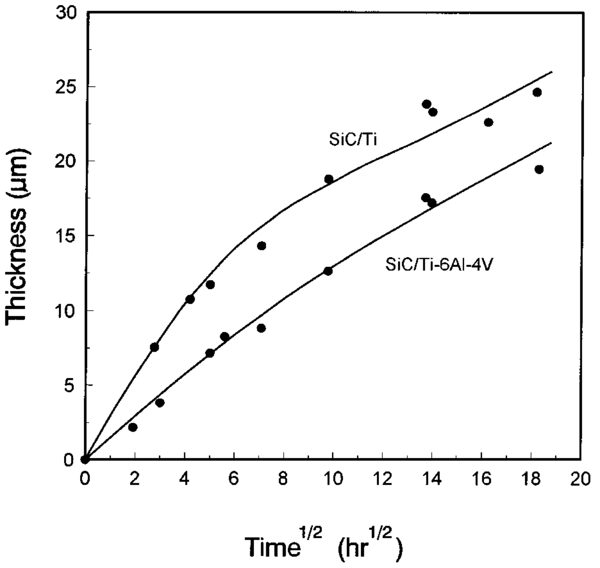

Figure 3 Interfacial layer growth in SiC/Ti-6Al-4V and SiC/Ti MMC's. (●) Experiment [1], (—) DPLD model.

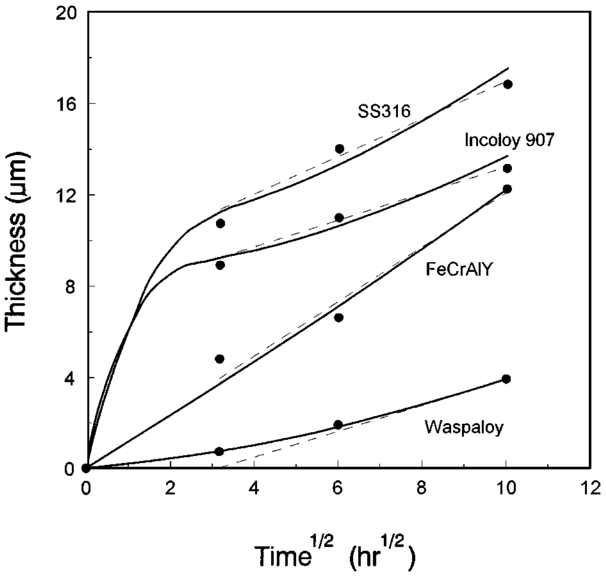

Figure 4 Intermetallic growth in W-fiber/superalloy MMC's. (●) Experiment [5], (- -) Prediction [5], (—) DPLD model.

using Fick's law. It is evident that Fick's law does not accurately simulate the RMILG. On the other hand, the DPLD model correlates well with the experimental result.

A comparison between the DPLD model and the experimental data of Martineau *et al.* [1] for the RMILG in both SiC/Ti-6Al-4V and SiC/Ti composites is shown in Fig. 3. The annealing temperatures are at 950 °C. Multiple-stage responses of the RMILG which cannot be fitted to a single straight line (Fick's law) within the whole $t^{1/2}$-axis for the two MMC's were reported in [1]. It is interesting to note the growth behaviors in relatively long and short times. The DPLD model predicts a linear response after time prolongs to about 200 h for SiC/Ti-6Al-4V and about 225 h for SiC/Ti. The linear growth behavior is also clearly seen at relatively short time in the case of SiC/Ti-6Al-4V. Again, there is a good agreement between the DPLD model and the measurements for the two cases.

Other examples of non-Fickian intermetallic growth are presented in Fig. 4. The composite specimens were annealed in vacuum at 1093 °C [5]. Each MMC consisted of the tungsten (W) fibers and a superalloy matrix. The W-fibers, doped with 1.5 wt % ThO_2 inert dispersoids, measured approximately 101 μm in initial diameter. Four superalloy matrices used were stainless steel 316, Incoloy 907, Fe-Cr-Al-Y and Waspaloy. The contents of these superalloys are given in [5].

The dashed lines, ranging over the experimental data, are the linear (Fick's law) predictions [5]. As shown in the figure, both the linear solutions and the DPLD model match well with the experimental data. Since only three data points were given here for each case, we are reluctant to conclude the DPLD model has precisely characterized the entire RMILG history. However, it is certain that the linear solutions are unable to predict the RMILG for short time. This can be seen by extrapolating the results to $t = 0$. Also note that the difference between the linear solutions and DPLD predictions will become larger and larger as time lengthens.

6. Conclusions

A one-dimensional DPLD model, which accounts for the different times required for the processes of interdiffusion and chemical reaction, is developed for simulating the growth of interfacial phase in MMC's. This model predicts the linear growth kinetics (H vs. $t^{1/2}$) but with different growth rates for relatively short and long times and captures the anomalous transition behavior in between. When the times for the interdiffusion and chemical reaction are identical, the model simplifies to Fick's law. In the model validation with seven different MMC systems, it is demonstrated that the DPLD model can be a robust and viable tool in the analysis of interfacial phase growth.

References

1. P. MARTINEAU, R. PAILLER, M. LAHAYE and R. NASLAIN, *J. Mater. Sci.* **19** (1984) 2749.
2. I. W. HALL, J. L. LIRN, Y. LEPETITCORPS and K. BILBA, *ibid.* **27** (1992) 3835.
3. C. A. BLUE, V. K. SIKKA, R. A. BLUE and R. Y. LIN, *Metall. Mater. Trans. A* **27A** (1996) 4011.
4. T. CAULFIELD and J. K. TIEN, *Metall. Trans. A.* **20A** (1989) 255.
5. J. K. TIEN, T. CAULFIELD and Y. P. WU, *ibid.* **20A** (1989) 267.
6. F. L. MATTHEWS and R. D. RAWLINGS, "Composite Materials: Engineering and Science" (Chapman & Hall, London, 1994) p. 87.
7. T. D. BAYHA and F. E. WAWNER, *Metall. Trans. A* **23A** (1992) 1607.
8. D. Y. TZOU, Y. XU and J. K. CHEN, submitted to *Int. J. Heat and Mass Transfer.*
9. J. K. CHEN, J. E. BERAUN and D. Y. TZOU, submitted to *Metall. Mater. Trans. A.*
10. F. P. INCROPERA and D. P. DEWITT, "Fundamentals of Heat and Mass Transfer" (Wiley, New York, 1985).
11. D. Y. TZOU, M. N. ÖZISIK and R. J. CHIFFELLE, *Int. J. Heat and Mass Transfer* **116** (1994) 1034.

Received 28 May 1997
and accepted 18 June 1999